

Modeling and optimizing the performance of a passive direct methanol fuel cell

Tsung-Kuang Yeh*, Chih-Hao Chen

Nuclear Science and Technology Development Center, National Tsing Hua University, Taiwan

Received 2 August 2007; received in revised form 11 September 2007; accepted 11 September 2007

Available online 14 September 2007

Abstract

Passive direct methanol fuel cells (DMFCs) are promising energy sources for portable electronic devices. Different from DMFCs with active fuel feeding systems, passive DMFCs with nearly stagnant fuel and air tend to bear comparatively less power densities. In the aspect of cell performance optimization, there could be significant differences in cell design parameters between active and passive DMFCs. A numerical model that could simulate methanol permeation and the pertinent mixed potential effect in a DMFC was used to help seek for possibilities of optimizing the cell performance of a passive DMFC by studying impacts from variations of cell design. The subjects studied include catalysis of the anode and the cathode, membrane thickness, membrane conductivity, and methanol concentration. In contrast to general understandings on a DMFC with active fuel and reactant gas, our simulation results for a passive DMFC used in this study indicated that the catalysis of the cathode appeared to be the most important parameter. The maximum power density was predicted to improve by 38% with the thickness of the cathodic catalyst layer doubled and by 36% with the catalyst loading doubled. The improvement on cell performance would multiply if we simultaneously adopted the most optimal parameters during the simulation study.

© 2007 Elsevier B.V. All rights reserved.

Keywords: Passive direct methanol fuel cell; Simulation; Catalysis; Anode; Cathode; Membrane

1. Introduction

The advantages of direct methanol fuel cells (DMFC) over hydrogen fuel cells include easy storage of the high energy density liquid fuel, direct fuel feeding without reforming, and low operating temperature. It is therefore considered by many people as the most promising alternative power source for mobile applications and electric vehicles. On the other hand, passive DMFCs are promising energy sources for portable electronic devices. Different from DMFCs with active fuel feeding systems, passive DMFCs with nearly stagnant fuel and air tend to bear comparatively less power densities. In the aspect of cell performance optimization, there could be significant differences in cell design parameters between active and passive DMFCs.

Performance of a DMFC relies on a vast number of parameters, including the methanol feed concentration, efficiencies of methanol transport and oxygen transport within the compart-

ments, the release rate of gaseous CO₂ and its effect on methanol transport, the specific area of catalyst in the catalyst layers, the thickness of the compartments, the impedance of the catalyst layer, the impedance of the membrane, the design of flow channels, the rate of methanol permeation and so on. Investigating the impact of these parameters one by one through experiments is not time or cost efficient. In order to help understand the operation of a DMFC and locate the key parameters on cell performance, a theoretical model is essential.

Numerous models were found in the literature [1–11], but the mixed potential effect was unaddressed, calculated in an empirical way, or handled with a simple assumption that the methanol that permeates the PEM is fully depleted at the cathode. Empirical approaches are often useful in correlating experimental data if the model contains sufficient insights of the system, but are less helpful on the investigation of cell parameters or on the effects of changing cell designs. We have proposed a mathematical model [12] which is based upon the description of the physicochemical processes dictating the behavior of electrochemical systems, namely, mass transport and reaction kinetics. One of the major discoveries is that the assumption of full depletion

* Corresponding author. Tel.: +886 3 5742864; fax: +886 3 5735441.
E-mail address: tkyeh@mx.nthu.edu.tw (T.-K. Yeh).

Nomenclature

A_{cell}	cell area
$C_{\text{CH}_3\text{OH}}$	local methanol concentration
$C_{\text{H}_2\text{O}}$	local water concentration
C_{O_2}	local oxygen concentration
$C_{\text{CH}_3\text{OH}}^{\text{feed}}$	methanol feed concentration
$C_{\text{O}_2}^{\text{feed}}$	oxygen feed concentration
$C_{\text{CH}_3\text{OH}}^{\text{ref}}$	reference methanol concentration
$C_{\text{O}_2}^{\text{ref}}$	reference oxygen concentration
$C_{\text{CH}_3\text{OH}}^{\text{vap}}$	gaseous methanol concentration at saturated vapor pressure
d_{af}	width of the anodic flow channel
d_{cf}	width of the cathodic flow channel
$D_{\text{CH}_3\text{OH},\text{H}_2\text{O}}$	bulk diffusion coefficient of methanol in water
$D_{\text{CH}_3\text{OH},\text{air}}$	bulk diffusion coefficient of gaseous methanol in air
$D_{\text{CH}_3\text{OH},\text{PEM}}$	diffusion coefficient of methanol in PEM
$D_{\text{O}_2,\text{air}}$	bulk diffusion coefficient of oxygen in air
$D_{\text{CH}_3\text{OH},\text{H}_2\text{O}}^{\text{ac,eff}}$	effective diffusion coefficient of methanol in the anodic catalyst layer
$D_{\text{CH}_3\text{OH},\text{H}_2\text{O}}^{\text{cc,eff}}$	effective diffusion coefficient of methanol in the cathodic catalyst layer
$D_{\text{O}_2,\text{air}}^{\text{cc,eff}}$	effective diffusion coefficient of oxygen in the cathodic catalyst layer
$D_{\text{CH}_3\text{OH},\text{H}_2\text{O}}^{\text{d,eff}}$	effective diffusion coefficient of methanol in diffusion layers
$D_{\text{O}_2,\text{air}}^{\text{d,eff}}$	effective diffusion coefficient of oxygen in diffusion layers
E	difference of electrode potentials in a DMFC
F	Faraday's constant
f_{af}	methanol flow rate in anodic flow channel
f_{cf}	air flow rate in cathodic flow channel
j_{O_2}	local current density from oxygen reduction
$j_{0,\text{CH}_3\text{OH}}^{\text{a,ref}}$	reference exchange current density of methanol in the anode
$j_{0,\text{CH}_3\text{OH}}^{\text{c,ref}}$	reference exchange current density of methanol in the cathode
$j_{0,\text{O}_2}^{\text{c,ref}}$	reference exchange current density of oxygen in the cathode
$j_{\text{cell}}^{\text{e}}$	cell external current density
$j_{\text{CH}_3\text{OH}}^{\text{e}}$	local external current density from methanol oxidation
$j_{\text{O}_2}^{\text{e}}$	local external current density from oxygen reduction
$j_{\text{cell}}^{\text{i}}$	cell internal current density
l_{af}	thickness of the anodic flow channel
l_{ac}	thickness of the anodic catalyst layer
l_{ad}	thickness of the anodic diffusion layer
l_{cc}	thickness of the cathodic catalyst layer
l_{cd}	thickness of the cathodic diffusion layer
l_{cf}	thickness of the cathodic flow channel
l_{m}	thickness of the PEM

$l_{\text{CH}_3\text{OH}}^{\text{a,ref}}$	reference catalyst layer thickness for methanol in the anode
$l_{\text{CH}_3\text{OH}}^{\text{c,ref}}$	reference catalyst layer thickness for methanol in the cathode
$l_{\text{O}_2}^{\text{c,ref}}$	reference catalyst layer thickness for oxygen in the cathode
$M_{\text{CH}_3\text{OH}}$	molecular weight of methanol
$M_{\text{H}_2\text{O}}$	molecular weight of water
$n_{\text{CH}_3\text{OH}}$	number of transferred electrons per methanol molecule
n_{O_2}	number of transferred electrons per water molecule
$N_{\text{CH}_3\text{OH}}$	local methanol flux
$N_{\text{H}_2\text{O}}$	local water flux
N_{O_2}	local oxygen flux
$r_{\text{cell}}^{\text{i}}$	cell interfacial resistance
V_{cell}	cell output voltage
$w_{\text{CH}_3\text{OH},\text{a}}$	decay width of methanol concentration along the anodic flow channel
$w_{\text{CH}_3\text{OH},\text{c}}$	decay width of methanol concentration along the cathodic flow channel
$w_{\text{O}_2,\text{c}}$	decay width of oxygen concentration along the cathodic flow channel

Greek letters

$\alpha_{\text{a},\text{CH}_3\text{OH}}^{\text{a}}$	anodic transfer coefficient of methanol in the anode
$\alpha_{\text{a},\text{CH}_3\text{OH}}^{\text{c}}$	anodic transfer coefficient of methanol in the cathode
$\alpha_{\text{c},\text{CH}_3\text{OH}}^{\text{a}}$	cathodic transfer coefficient of methanol in the anode
$\alpha_{\text{c},\text{CH}_3\text{OH}}^{\text{c}}$	cathodic transfer coefficient of methanol in the cathode
$\alpha_{\text{a},\text{O}_2}^{\text{c}}$	anodic transfer coefficient of oxygen in the cathode
$\alpha_{\text{c},\text{O}_2}^{\text{c}}$	cathodic transfer coefficient of oxygen in the cathode
ε^{d}	void fraction of diffusion layers
$\varepsilon_{\text{s}}^{\text{ac}}$	volume fraction of solid phase in anodic catalyst layer
$\varepsilon_{\text{s}}^{\text{cc}}$	volume fraction of solid phase in cathodic catalyst layer
$\varepsilon_{\text{m}}^{\text{c}}$	volume fraction of ionomer phase in catalyst layers
$\gamma_{\text{CH}_3\text{OH}}^{\text{a}}$	reaction order of methanol in the anode
$\gamma_{\text{CH}_3\text{OH}}^{\text{c}}$	reaction order of methanol in the cathode
$\gamma_{\text{O}_2}^{\text{c}}$	reaction order of oxygen in the cathode
γ_{O_2}	reaction order of oxygen
$\eta_{\text{CH}_3\text{OH}}^{\text{e}}$	local external overpotential of methanol
$\eta_{\text{O}_2}^{\text{e}}$	local external overpotential of oxygen
$\kappa_{\text{s}}^{\text{ac,eff}}$	effective conductivity of solid phase in the anodic catalyst layer
$\kappa_{\text{s}}^{\text{cc,eff}}$	effective conductivity of solid phase in the cathodic catalyst layer

$\kappa_m^{c,eff}$	effective conductivity of ionomer phase in catalyst layers
κ_s^{ac}	conductivity of solid phase in the anodic catalyst layer
κ_s^{cc}	conductivity of solid phase in the cathodic catalyst layer
κ_m^c	conductivity of ionomer phase in catalyst layers
κ_m	specific conductivity of the PEM
λ_{H_2O}	drag coefficient of water
ρ_{CH_3OH}	density of methanol
ρ_{H_2O}	density of water

of the permeating methanol may not always be true, especially when catalysis of the cathode is not so efficient. Therefore, calculation of the mixed potential effect based on this assumption is not always reliable. In this study, we go one step further to demonstrate the capability of this model by seeking possibilities to optimize the performance of an air-breathing, passive DMFC. With the increasing attempts of putting DMFCs into portable electronic devices, passive DMFCs of low power density are drawing more attention. Due to differences in feeding mode of the fuel and the reactant gas, optimal design parameters used in a dynamic DMFC may not be suitable for a passive DMFC since the methanol oxidation and oxygen reduction efficiencies at both electrodes may be markedly different. Modeling work for the passive DMFC on the effect of methanol concentration was reported by Chen and Zhao, but no parametric studies were conducted [13]. Parameters other than the methanol concentration are speculated to influence the performance of a passive DMFC to an equivalent or even more extent.

In the current study we focus on the following parameters which we think are the most significant ones to cell performances: catalysis, PEM characteristics, methanol feed concentration. In general, catalysis can be improved in two different ways, increasing the thickness of the catalyst layer or increasing the catalyst loading. The former one would induce an addition to the ohmic (IR) loss and the latter might induce catalyst aggregation and thus reduce the efficiency. The thickness and the conductivity of the PEM play major roles in cell performances. Thickening the PEM is expected to reduce the methanol permeation rate and thus alleviate the mixed potential effect. However, with its low conductivity, this approach may not be feasible since it induces a higher IR loss. A higher methanol concentration would lead to higher concentrations of reacting species within the catalyst layer and hence a greater cell current density. This is true only when methanol permeation from the anode to the cathode does not occur. As pointed out in our earlier work, the mixed potential effect due to methanol permeation is overwhelming. In contrast to a dynamic DMFC in which the fuel feeding at the anode is generally operated by an external pump, a passive DMFC could experience a different degree of mixed potential effect due to its stagnant fuel or extremely slow fuel transport by gravity or capillary force. In the presence of the foregoing variables and the possible combined effects, a

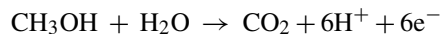
full simulation is required to understand the total impact since detailed analyses by physical experiments would be relatively time-consuming and inefficient.

In this work, we selected an in-house passive DMFC constructed with known and estimated parameters as a base cell to calibrate our model. Modeling work then started with various parameters such as catalyst loadings, catalyst layer thickness, PEM thickness, and methanol concentrations. The impacts of these parameters individually or in combination on the efficiency of the passive DMFC were analyzed and discussed.

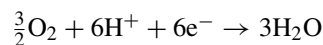
2. Theory and modeling procedures

Since the mathematical model has been presented in details in [12], only a brief description is given in this paper.

As shown schematically in Fig. 1, the structure a DMFC consists of seven major compartments namely the anodic flow channel, the anodic diffusion layer, the anodic catalyst layer, the proton exchange membrane (PEM), the cathodic catalyst layer, the cathodic diffusion layer and the cathodic flow channel. The anodic flow channel is the passage of low concentration methanol solution. As the solution is pumped through the channel, a small fraction of methanol diffuses through the anodic diffusion layer and reaches the anodic catalyst layer. Within this layer, where Pt-Ru is the most widely used catalyst today, methanol oxidizes and produces carbon dioxide (CO_2) via the following reaction:



CO_2 then diffuses back into the anodic flow channel and exits with the solution. The protons, which travel through the PEM, and the electrons, which travel through some external load, reach the cathodic catalyst layer, where Pt is the catalyst, to undergo the following half-cell reaction with oxygen that comes from the cathodic flow channel:



The overall reaction can therefore be written as:

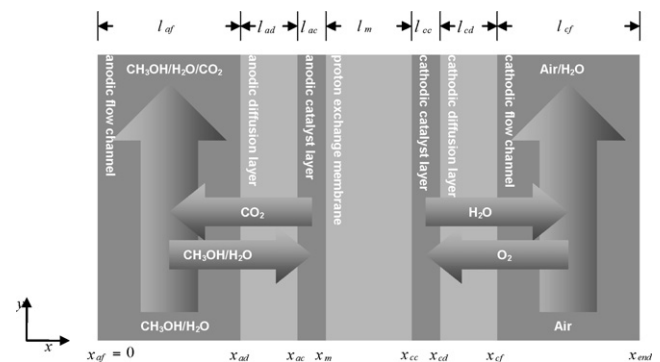
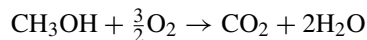


Fig. 1. Schematic of the DMFC which is divided into seven compartments namely the anodic flow channel, the anodic diffusion layer, the anodic catalyst layer, the PEM, the cathodic catalyst layer, the cathodic diffusion layer and the cathodic flow channel.

Despite its advantages over hydrogen fuel cells, a few engineering obstacles of the DMFC remain to overcome. On the one hand, the sluggish catalytic activity of the anode makes a higher methanol concentration favorable. On the other hand, the methanol permeation problem, which does not exist in hydrogen fuel cells, generates a mixed potential at the cathode and adversely lowers the cell output voltage at higher methanol concentration. Another important issue is that methanol transport may be hindered by CO₂ that diffuses back into the anodic flow channel after being released within the anodic catalyst layer.

In this work, the term ‘external currents’ refers to currents that go through external load and ‘internal currents’ to currents that do not. How methanol permeation influences the performance of a DMFC is explained in the following. The cell output voltage V is related to the potential differential difference E by:

$$V = E - \eta_a - \eta_c - IR$$

where η_a and η_c are the activation overpotentials of the anode and the cathode, respectively, and IR is the ohmic loss. Assume the cathodic catalyst layer is of zero thickness, η_c is related to the internal current density i^i and the external current density i^e by the following Butler-Volmer equation:

$$i_i + i_e = i_0 \left[\exp \left(\frac{\eta_c}{b_a} \right) - \exp \left(\frac{\eta_c}{b_c} \right) \right]$$

where i_0 is the exchange current density of oxygen, and b_a and b_c are the Tafel slopes of oxygen oxidation and reduction, respectively. If we keep i^e constant and raise i^i , η_c will be raised and therefore V will be lowered. Because contributions from i^i and i^e to η_c are mixed together and cannot be separated, η_c is usually referred to as the mixed potential.

In addition to the conditions described above, our model is also based on the following set of assumptions:

1. The fuel cell is operated isothermally at 30 °C in a steady state.
2. There is no pressure difference between the compartments.
3. Methanol flux into the anodic flow channel is much greater than methanol flux into the anodic diffusion layer. This ensures that methanol concentration variation is small along the channel. The same assumption applies to oxygen flux in the cathodic flow channel.
4. The effects of generated products, carbon dioxide and water, on methanol transport and on oxygen transport are neglected.

In our model, mass transport of water, methanol and oxygen are considered all over the cell. Within the flow channels, mass transport of methanol and oxygen are accounted for by considering fluid dynamics. Water transport is driven by electro-osmotic drag. The consumption of water in the anodic catalyst layer and the creation of it in the cathodic catalyst layer have been accounted for. Methanol transport is driven by diffusion and convection and is considered in all seven compartments of the cell. Methanol is assumed to evaporate at the boundary of the cathodic

diffusion layer and the cathodic flow channel, and to exist in the cathodic flow channel in gas phase. Oxygen is assumed to exist only in the cathode and its transport is driven by diffusion only. Methanol oxidation is considered in both the anode and the cathode, but oxygen reduction is considered only in the cathode. The electrochemical reaction rates for both the external currents and the internal currents are quantified by appropriate kinetic Tafel expressions. With the physics given above, a set of differential equations can be derived. An appropriate set of boundary conditions can also be derived by considering methanol feed concentration in the anodic flow channel, oxygen feed concentration in the cathodic flow channel, continuation of concentrations and flux across every boundary and methanol evaporation at the boundary of the cathodic diffusion layer and the cathodic flow channel. The problem can then be

Table 1
Parameter values for the in-house passive direct methanol fuel cell

Parameter	Value	Reference
A_{cell} (cm ²)	4	Measurement
$D_{\text{CH}_3\text{OH},\text{H}_2\text{O}}$ (cm ² s ⁻¹)	1.93×10^{-5}	[14]
$D_{\text{CH}_3\text{OH},\text{air}}$ (cm ² s ⁻¹)	1.569×10^{-1}	[15]
$D_{\text{CH}_3\text{OH},\text{PEM}}$ (cm ² s ⁻¹)	4.9×10^{-6}	[8]
$D_{\text{O}_2,\text{air}}$ (cm ² s ⁻¹)	1.02×10^1	[14]
d_{af} (cm)	0.1	Measurement
d_{cf} (cm)	0.1	Measurement
f_{af} (cm ³ s ⁻¹)	0	Measurement
f_{cf} (cm ³ s ⁻¹)	0	Measurement
$J_{0,\text{CH}_3\text{OH}}^{\text{a,ref}}$ (A cm ⁻²)	4.5×10^{-4}	Calibration
$J_{0,\text{CH}_3\text{OH}}^{\text{c,ref}}$ (A cm ⁻²)	4.5×10^{-4}	Calibration
$l_{\text{CH}_3\text{OH}}^{\text{a,ref}}$ (cm)	0.03	Measurement
$l_{\text{CH}_3\text{OH}}^{\text{c,ref}}$ (cm)	0.03	Measurement
$J_{0,\text{O}_2}^{\text{c,ref}}$ (A cm ⁻²)	1×10^{-4}	Calibration
$l_{\text{O}_2}^{\text{c,ref}}$ (cm)	0.03	Measurement
l_{af} (cm)	0.1	Measurement
l_{ad} (cm)	0.03	Measurement
l_{ac} (cm)	0.001	Measurement
l_{m} (cm)	0.015	Measurement
l_{cc} (cm)	0.001	Measurement
l_{cd} (cm)	0.03	Measurement
l_{cf} (cm)	0.1	Measurement
r_{cell}^i (ohm)	1.4	Calibration
$\alpha_{\text{a,CH}_3\text{OH}}^{\text{a}}$	0.153	Calibration
$\alpha_{\text{a,CH}_3\text{OH}}^{\text{c}}$	0.153	Calibration
$\alpha_{\text{c,CH}_3\text{OH}}^{\text{a}}$	0.12	Calibration
$\alpha_{\text{c,CH}_3\text{OH}}^{\text{c}}$	0.12	Calibration
$\alpha_{\text{a,O}_2}^{\text{c}}$	0.0669	Assumption
$\alpha_{\text{c,O}_2}^{\text{c}}$	0.0669	[9]
$\gamma_{\text{CH}_3\text{OH}}^{\text{a}}$	1.4	Calibration
$\gamma_{\text{CH}_3\text{OH}}^{\text{c}}$	2	Calibration
$\gamma_{\text{O}_2}^{\text{c}}$	1	Calibration
$\kappa_{\text{s}}^{\text{ac}}$ (S cm ⁻¹)	8.13×10^6	[10]
$\kappa_{\text{s}}^{\text{cc}}$ (S cm ⁻¹)	8.13×10^6	Assumption
$\kappa_{\text{m}}^{\text{c}}$ (S cm ⁻¹)	1.416×10^{-1}	[8]
$\kappa_{\text{m}}^{\text{m}}$ (S cm ⁻¹)	8.3×10^{-2}	[11]
ε^{d}	7.06×10^{-1}	[2]
$\varepsilon_{\text{s}}^{\text{ac}}$	6×10^{-1}	[2]
$\varepsilon_{\text{s}}^{\text{cc}}$	6×10^{-1}	Assumption
$\varepsilon_{\text{m}}^{\text{c}}$	8×10^{-2}	[2]
$\lambda_{\text{H}_2\text{O}}$	2.36	[7]

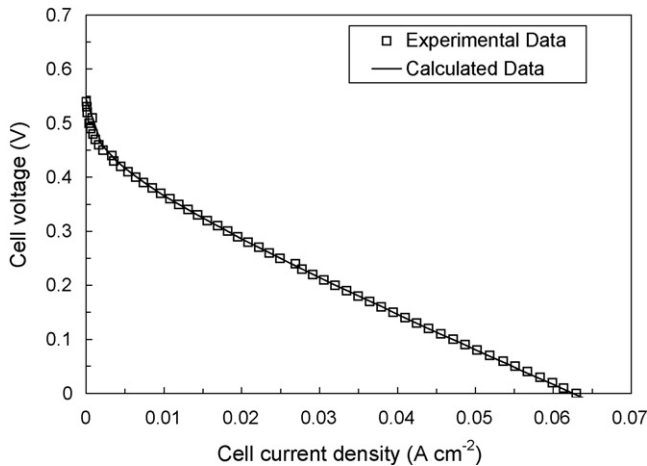


Fig. 2. Experimental and calculated polarization curves of the passive DMFC operating at 25 °C under atmospheric pressure.

solved by applying Runge-Kutta methanol of order four. The concentrations and flux of the species all over the cell along with their reaction rates within the catalyst layers can be known. The cell output voltage can then be estimated by considering conservations of power density. Detailed governing equations and theoretical bases adopted in this model can be found in our earlier work [12] and are not discussed in this paper.

The features that distinguish our model from the other models available in the literature [1–6] are:

1. fluid dynamics of the flow channels which may influence the concentrations of species at the catalyst layers, change the reaction rates and impact the performance of the cell,
2. mass transport and reaction kinetics of the cathode, and

3. a means to estimating the intensity of the internal current, the mixed potential effect and consequently the impact on cell output voltage.

A case study is performed on the basis of the particular cell we assembled in our laboratory [12] of which the parameter values are listed in Table 1 [7–11,14,15] and the polarization curve is shown in Fig. 2. This passive DMFC was an air-breathing one using 1 M static methanol solution at the anode, and the Pt loadings at both the anode and the cathode were the same at 0.9 mg cm^{-2} . With the relatively low catalyst loadings, it could only generate a maximum power density of 6.3 mW cm^{-2} at 25 °C under atmospheric pressure. The major aim of this work is therefore to determine through theoretical analyses the most appropriate approach that would effectively elevate the power density of this passive DMFC.

Modeling variables studied included the catalyst loadings and layer thickness at the anode and the cathode, the PEM thickness and conductivity, and the methanol concentration. Although the modeling work focused on an air-breathing DMFC, an additional design parameter of air feeding rate at the cathode was taken into account to exemplify the benefit of using circulating air. In fact, dynamic air feeding is possible to engineer if the passive DMFC is adopted in a laptop computer or some other electronic device with an internal cooling fan. In addition, a case of combined, optimal parameters was also modeled. All the cases are listed in Table 2 along with their respective descriptions. Case CONTROL is defined to assume the parameter values of Table 1, a methanol concentration of 1 M and an air pressure of 1 atm. Experiments on evaluating the impact of the foregoing parameters on the performance of various passive DMFCs have been carried out by several laboratories around the

Table 2
Descriptions and effects of the cases in the current case study

Case	Description	Effect on maximum power density (%)
CONTROL	Assumes the parameter values of Table 1, methanol feed concentration is 1 M, air feed pressure is 1 atm	0
ACLLD	The loading of the anodic catalyst layer is decreased by a factor of 0.5	–9
ACLLU	The loading of the anodic catalyst layer is increased by a factor of 2	7
ACLTD	The thickness of the anodic catalyst layer is decreased by a factor of 0.5	–9
ACLTU	The thickness of the anodic catalyst layer is increased by a factor of 2	9
CCLLD	The loading of the cathodic catalyst layer is decreased by a factor of 0.5	–27
CCLLU	The loading of the cathodic catalyst layer is increased by a factor of 2	36
CCLTD	The thickness of the cathodic catalyst layer is decreased by a factor of 0.5	–26
CCLTU	The thickness of the cathodic catalyst layer is increased by a factor of 2	38
PEMTU1	The thickness of the PEM is increased by a factor of 2	14
PEMTU2	The thickness of the PEM is increased by a factor of 4	24
PEMTU3	The thickness of the PEM is increased by a factor of 8	26
PEMTU4	The thickness of the PEM is increased by a factor of 16	18
PEMCD	The conductivity of the PEM is decreased by a factor of 0.5	–2
PEMCU	The conductivity of the PEM is increased by a factor of 0.5	1
MFCD1	The methanol feed concentration is decreased by a factor of 0.5	9
MFCD2	The methanol feed concentration is decreased by a factor of 0.25	5
MFCD3	The methanol feed concentration is decreased by a factor of 0.125	–16
MFCU	The methanol feed concentration is increased by a factor of 2	–14
AFPU1	An air feeding rate of $3.32 \text{ cm}^3 \text{ s}^{-1}$ was adopted	36
AFPU2	An air feeding rate of $6.64 \text{ cm}^3 \text{ s}^{-1}$ was adopted	80
COMBINATION	ACLLU + CCLLU + PEMTU3 + MFCD1 + AFPU2	140

world [16–18], and the test results were employed to compare with our modeling results qualitatively.

Unless otherwise specified, each of the other cases differs from case CONTROL in only one parameter by a factor of an exponent of 2. Plots of current–voltage (I – V) characteristic curves and power density curves are made to appraise the impacts of these cell design changes on cell performance.

3. Results and discussion

The impacts of design parameters on the efficiency of the passive DMFC are evaluated via the calculated peak power densities. These design parameters were varied to account for the effects resulted from changes in catalytic activity, PEM characteristics, fuel concentration, and air feeding pressure. The results of these cases are discussed as follows.

3.1. Catalysis

Catalysis improvement is one of the major goals of current DMFC development. For both the anode and the cathode, better catalysis means a lower activation overpotential and a higher operating cell voltage, and it can be achieved either by increasing specific catalyst loading or by increasing the thickness of the catalyst layer.

Both approaches would increase the total amount and hence the total active area of the catalyst at the electrode. However, the first approach does not affect the IR loss much and may improve the exchange current densities significantly until severe catalyst aggregation occurs. The second approach would lead to more active sites of the catalyst layer without causing catalyst aggregation but could induce a higher IR loss due to increased thickness. To better understand the effects of these approaches, we define and study the following cases: ACLLD and ACLLU for the anodic catalyst loading, ACLTD and ACLTU for the thickness of the anodic catalyst layer, CCLLD and CCLLU for the cathodic catalyst loading, and CCLTD and CCLTU for the thickness of the cathodic catalyst layer.

The results are shown in Figs. 3 and 4 and Table 2. The passive DMFC selected in this study was an air-breathing one using 1 M static methanol solution at the anode, and it could generate a current density of 30 mA cm^{-2} at an operating voltage of 0.21 V (leading to a maximum power density of 6.3 mW cm^{-2}) at 25°C under atmospheric pressure, as shown in Fig. 2. In the same figure it is noted that the polarization curve of case CONTROL had been calibrated with the experimental data of the selected DMFC. Due to the low cell current densities, the two approaches mentioned above yield very similar effects on both the anode and the cathode. A higher catalyst loading or a thicker

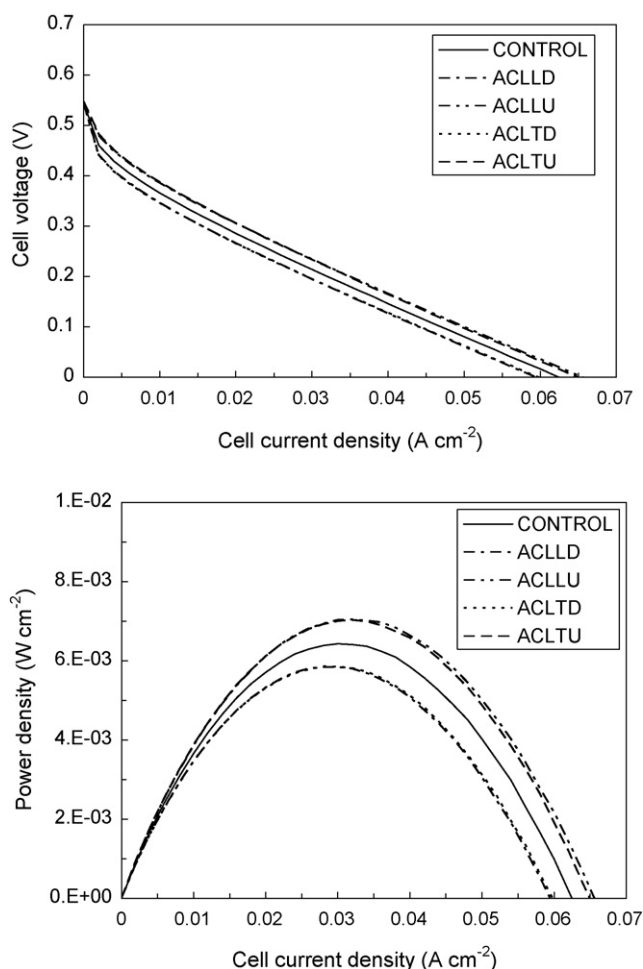


Fig. 3. I – V characteristic curves and power densities of cases of different catalysis of the anode.

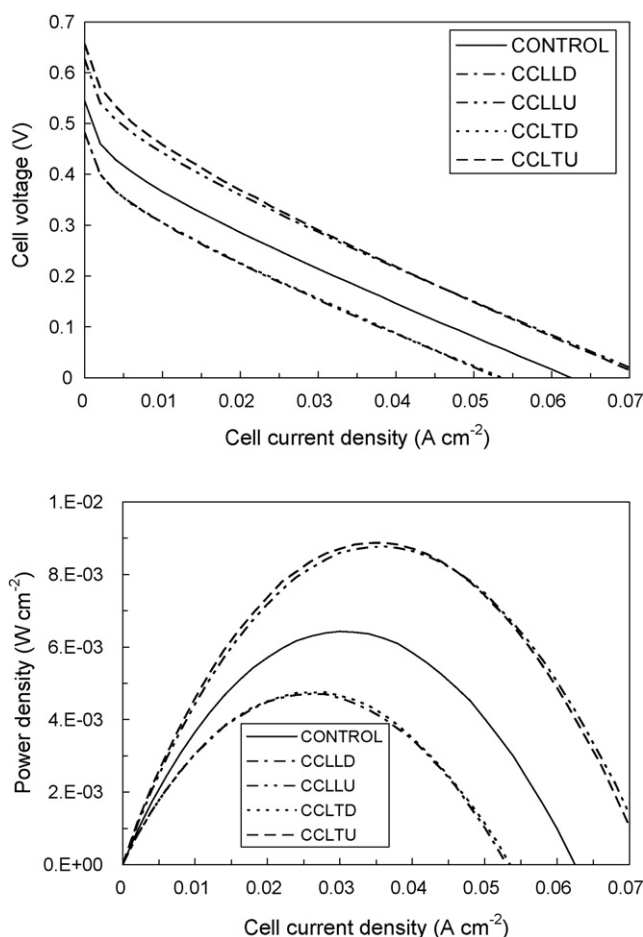


Fig. 4. I – V characteristic curves and power densities of cases of different catalysis of the cathode.

catalyst layer delivered a similar degree of improvement on cell efficiency. The IR loss did not play an important role when the thickness of the catalyst layer was increased by 100%. This is not surprising since the cell current density was relatively small in this passive DMFC. In particular, the catalysis of the cathode appeared to be comparatively more important. The maximum power density was improved by 38% with the thickness of the catalyst layer doubled and by 36% with the catalyst loading doubled at the cathode. The respective improvements at the anode were 7% and 9% only. For this particular passive DMFC, the catalyst loading at the cathode dominated the improvement in cell efficiency. Similar phenomena could be found in the experimental work by Bae [16] on investigating the effect of catalyst loading in the performance of a passive DMFC of low cell current density.

3.2. PEM characteristics

The thickness of the PEM plays a major role in the mixed potential effect which is responsible for adversely lowering the cell voltage especially when the methanol feed concentration is high. Thickening the PEM is expected to lower the methanol permeation rate and thus alleviate the mixed potential effect. However, the low conductivity of the PEM makes this approach

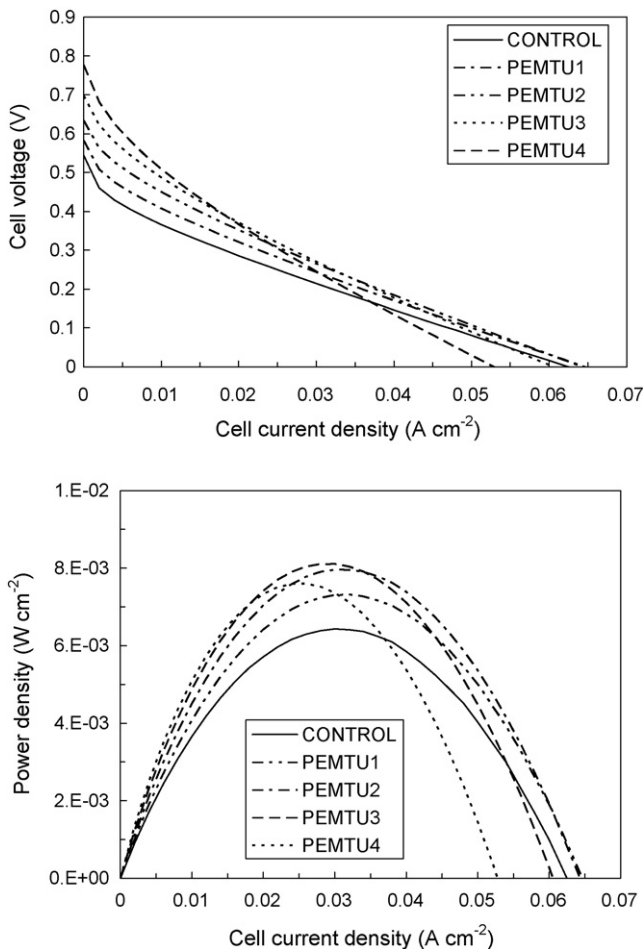


Fig. 5. I - V characteristic curves and power densities of cases of different thicknesses of the PEM.

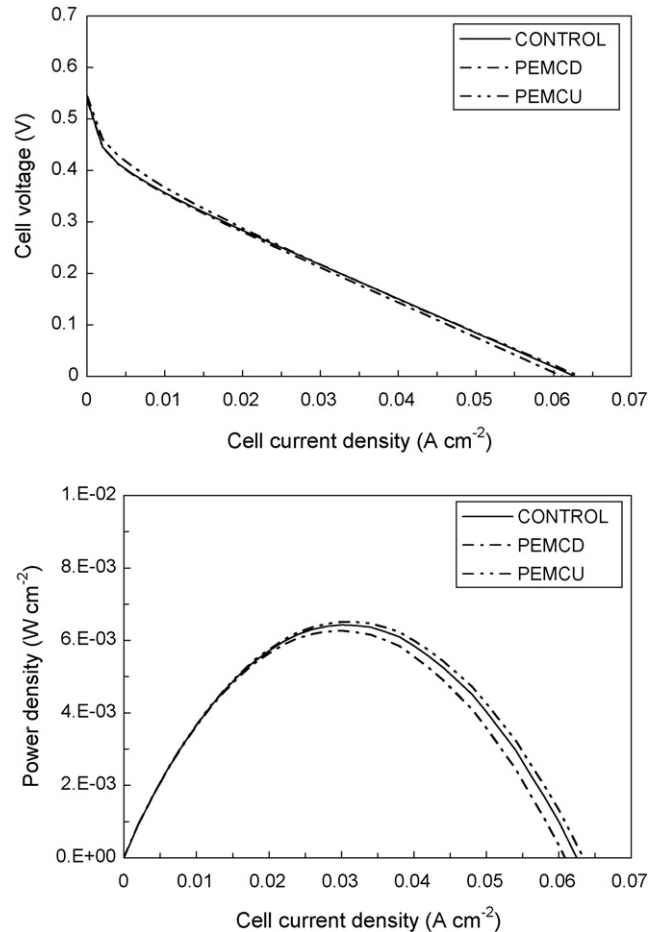


Fig. 6. I - V characteristic curves and power densities of cases of different conductivities of the PEM.

less feasible because of the induced addition to the already high IR loss. Therefore, we defined and studied the following cases to estimate the effects of varying the thickness and the conductivity of the PEM: PEMTU1, PEMTU2, PEMTU3 and PENTU4 for thickness variations of the PEM, PEMCD and PEMCU for conductivity variations of the PEM.

The results are shown in Figs. 5 and 6 and Table 2. Thickening the PEM improved the power densities before the IR loss became significant, as shown in Fig. 4. The optimal thickness is found to be about 0.12 cm, eight times as thick as that in case CONTROL. The maximum power density was promoted by 26% when this parameter was doubled. On the other hand, the maximum power density was increased by 18% when the PEM was further increased to 16 times as the original thickness. For a DMFC of low power density, this outcome is not surprising since methanol permeation from the anode to the cathode and the subsequent mixed potential effect dominated the cell voltage. Therefore, thickening the PEM actually promoted the cell efficiency by reducing the amount of permeating methanol and the impact of mixed potential effect at the cathode. The beneficial effect of a thicker membrane on the performance of a passive DMFC of low cell current density was also reported by Liu et al. [17] in their experimental work. In the meantime, due to the already low cell current densities, varying conductivity of the

PEM did not induce significant changes to the cell efficiency, as is also shown in Fig. 6.

3.3. Methanol concentration

Methanol concentration is more easily controllable than the other parameters in a laboratory. A higher concentration is favored if one only consider the anodic activation potential. However, if the mixed potential effect is taken into account, a higher concentration usually worsens the cell performance by lowering the cell voltage. This is particularly true when the methanol oxidation reaction rate (or the electrocatalytic activity of the catalyst) at the anode is not high enough and in turn leads to more methanol permeation to the cathode. For evaluating the effect of variations in methanol concentration on cell performance, we define and study the following cases: MFCD1, MFCD2, MFCD3 and MFCU with methanol concentrations of 0.5 M, 0.25 M, 0.125 M, and 2 M, respectively. The methanol concentration adopted in case CONTROL was 1 M.

Detailed results are shown in Fig. 7 and Table 2. For the selected passive DMFC, the mixed potential effect dominated the cell performance as mentioned earlier. At cell current densities less than 0.03 A cm^{-2} , lower methanol feed concentrations

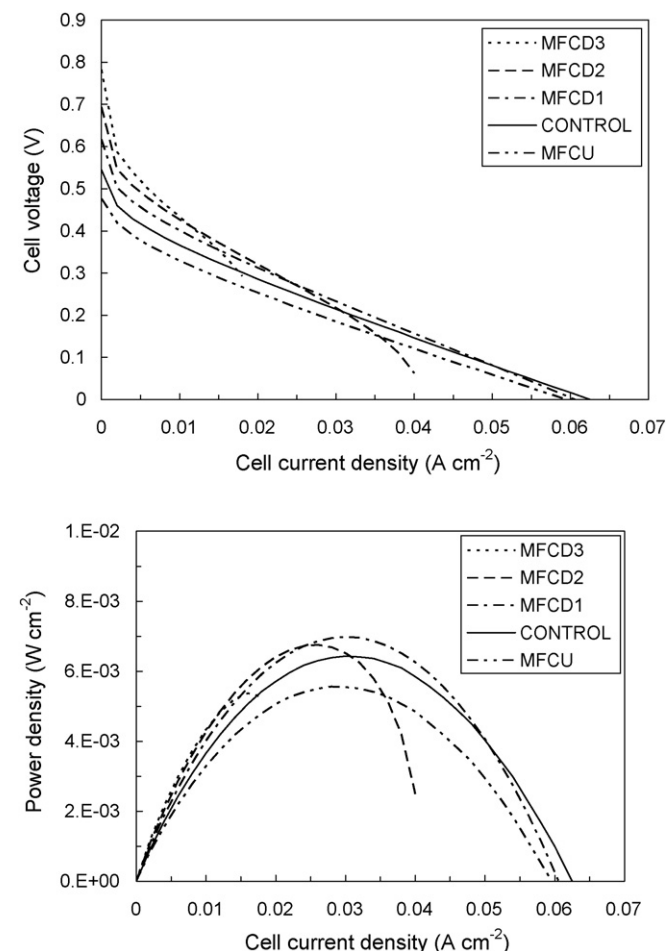


Fig. 7. I - V characteristic curves and power densities of cases of different methanol feed concentrations.

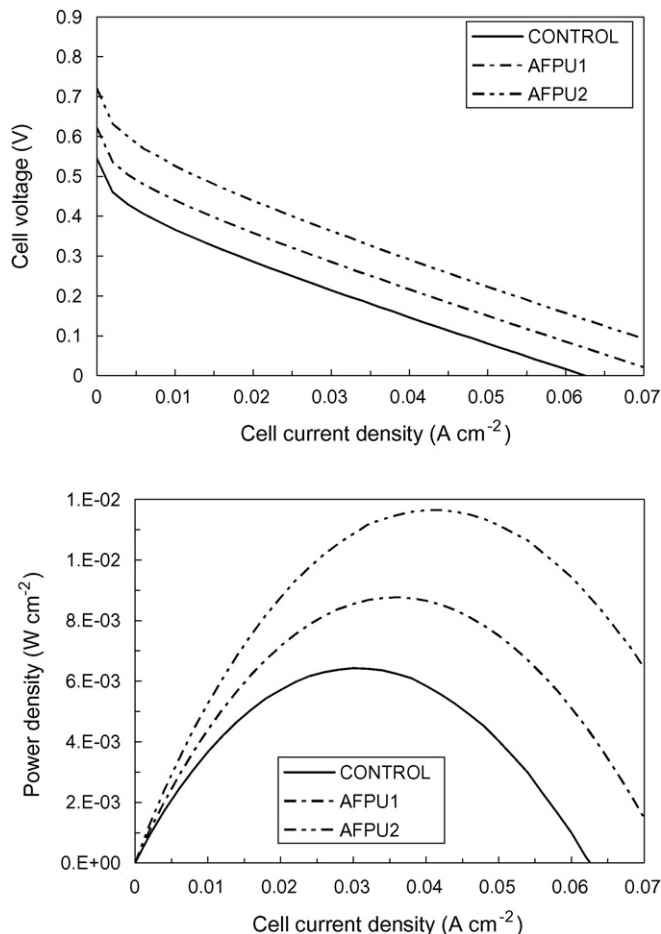


Fig. 8. I - V characteristic curves and power densities of cases of different air feed pressures.

yielded higher power densities before cell current densities became limited by methanol mass transfer. A higher methanol concentration of 2 M would instead lower the maximum power density of the cell by 14%. Our simulation results also indicated that the optimal methanol feed concentration for this particular cell was about 0.5 M at which the maximum power density was promoted by 9% without significantly sacrificing the cell current density.

3.4. Air feeding rate

Dynamic air feeding at the cathode is possible if the passive DMFC is adopted in an electronic device with an internal cooling fan. To investigate the effect of using dynamic air feeding instead of the air-breathing mechanism on the cell performance, we studied the following cases: AFPU1 and AFPU2. Air feeding rates of 3.32 and $6.64 \text{ cm}^3 \text{ s}^{-1}$ were assumed at the cathode. Simulation results, as shown in Fig. 8 and Table 2, indicated that the impact of dynamic air feeding was relatively significant. The maximum power densities of the selected DMFC were increased by 36% and 80%, respectively. The outcome was consistent with what had been observed in the case of increased catalyst loading at the cathode. Parameter changes at the cathode of this particular DMFC seemed to

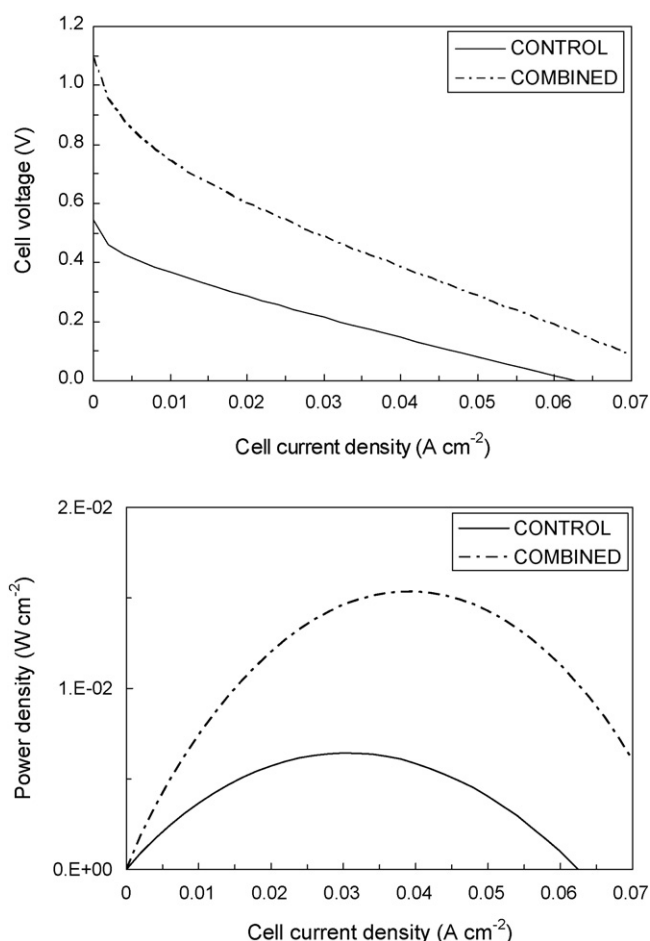


Fig. 9. I - V characteristic curves and power densities of case COMBINED and case CONTROL.

dominate the cell performance more efficiently than those in the PEM and those at the anode. Through experimental tests, Abdelkareem and Nakagawa [18] also found for a DMFC of low cell current density a dynamic air feeding rate tended to bear a distinctly better cell performance than an air-breathing one. This part of the simulation implicated that a coupling of an internal cooling fan with the cathode of an air-breathing DMFC could have a positively significant impact on the cell performance.

3.5. Combination of effects

According to the foregoing simulation results, the improvement on cell performance should multiply if we simultaneously adopt the most optimal parameters during the simulation study, that is, we double the catalyst loading of both the anode and the cathode, increase the thickness of the PEM by eight times, decrease the methanol concentration to 0.5 M, and adopt an air feeding rate of $6.64 \text{ cm}^3 \text{ s}^{-1}$. For verification, we define and study case COMBINED. Simulation results, as shown in Fig. 9 and Table 2, indicated that the maximum power density was promoted by an encouraging 140%.

To demonstrate the usefulness and function of our mathematical model on the search for key parameters for cell performance improvement, we performed a thorough case study for our laboratory-made passive DMFC on parameters of catalysis, PEM characteristics, methanol concentration and air feeding rate. With a useful tool such as this mathematical model, one would be able to determine the key design or environmental parameter that would significantly influence the performance of a DMFC, without going through complicated and tedious laboratory tests.

4. Conclusions

A mathematical model was used to analyze the performance of a passive DMFC and to determine a single key parameter or combined parameters that would promote its efficiency most effectively.

For the selected passive DMFC, the catalysis of the cathode appeared to be the most important parameter. The maximum power density was improved by 38% with the thickness of the cathodic catalyst layer doubled and by 36% with the catalyst loading doubled.

The improvement on cell performance would multiply if we simultaneously adopted the most optimal parameters during the simulation study.

The theoretical model may serve as a useful tool for determining key design or environmental parameters that would significantly influence the performance of a DMFC.

Acknowledgements

This research was sponsored by National Science Council and Institute of Nuclear Energy Research under contract numbers 94-2218-E-007-018 and 942001INER012, respectively. We would like to thank Mr. Chao-Yuan Chiang who conducted the experiment and provided the experimental data needed for this paper.

References

- [1] K. Scott, P. Argyropoulos, K. Sundmacher, *J. Electroanal. Chem.* 477 (1999) 97–110.
- [2] K.T. Jeng, C.W. Chen, *J. Power Sources* 112 (2002) 67–375.
- [3] J.P. Meyers, J.I. Newman, *J. Electrochem. Soc.* 149 (2002) A710–A717.
- [4] J. Divisek, J. Fuhrmann, K. Gärtner, R. Jung, *J. Electrochem. Soc.* 150 (2003) A811–A825.
- [5] Z.H. Wang, C.Y. Wang, *J. Electrochem. Soc.* 150 (2003) A508–A519.
- [6] J.J. Baschuk, X. Li, *J. Power Sources* 86 (2000) 181.
- [7] X. Ren, W. Handerson, S. Gottesfeld, *J. Electrochem. Soc.* 144 (9) (1997) L267.
- [8] K. Scott, W. Taama, J. Cruickshank, *J. Power Sources* 65 (1997) 159.
- [9] A. Parthasarathy, S. Srinivasan, A.J. Appleby, *J. Electrochem. Soc.* 139 (1992) 2530.
- [10] S.F. Baxter, V.S. Battaglia, R.E. White, *J. Electrochem. Soc.* 146 (2) (1999) 437.
- [11] T.A. Zawodzinski, M. Neeman, L.D. Sillerud, S. Gottesfeld, *J. Phys. Chem.* 95 (1991) 6040.
- [12] C.H. Chen, T.K. Yeh, *J. Power Sources* 160 (2006) 1131.
- [13] R. Chen, T.S. Zhao, *J. Power Sources* 152 (2005) 122.

- [14] E.L. Cussler, *Diffusion: Mass Transfer in Fluid Systems*, Cambridge University Press, New York, 1984.
- [15] C.L. Yaws, *Handbook of Transport Property Data: Viscosity, Thermal Conductivity, and Diffusion Coefficients of Liquids and Gases*, Gulf Pub Co., Houston, TX, 1995.
- [16] B. Bae, B.K. Kho, T.H. Lim, I.H. Oh, S.A. Hong, H.Y. Ha, *J. Power Sources* 158 (2006) 1256.
- [17] J.G. Liu, T.S. Zhao, Z.X. Liang, R. Chen, *J. Power Sources* 153 (2006) 61.
- [18] M.A. Abdelkareem, N. Nakagawa, *J. Power Sources* 165 (2007) 685.